



Review

Ferrite-based magnetic nanofluids used in hyperthermia applications

Ibrahim Sharifi, H. Shokrollahi*, S. Amiri

Electroceramics Group, Department of Materials Science and Engineering, Shiraz University of Technology, Shiraz, Iran

ARTICLE INFO

Article history:

Received 11 July 2011

Received in revised form

27 September 2011

Available online 28 October 2011

Keywords:

Ferrite

Hyperthermia

Magnetic property

Magnetic nanofluid

ABSTRACT

Magnetic ferrofluids (magnetic nanofluids) have received special attention due to their various biomedical applications such as drug delivery and hyperthermia treatment for cancer. The biological applications impose some special requirements. For example, the well-known iron oxide ferrofluids become undesirable because their iron atoms are poorly distinguishable from those of hemoglobin. A conceivable solution is to use mixed-ferrites (MFe_2O_4 where $M=Co, Mn, Ni, Zn$) to have a range of magnetic properties. These ferrites have attracted special attention because they save time, and because of their low inherent toxicity, ease of synthesis, physical and chemical stabilities and suitable magnetic properties. Based on the importance of ferrite particles in ferrofluids for hyperthermia treatment, this paper gives a summary on the physical concepts of ferrofluids, hyperthermia principal, magnetic properties and synthesis methods of nanosized ferrites.

© 2011 Elsevier B.V. All rights reserved.

1. Introduction

In any discussion of fluids with magnetic properties, it is convenient to divide them into the following categories: (A) ferrofluids; (B) magnetorheological fluids; (C) dispersions of micron-sized particles of a non-magnetic material containing magnetic nanosized particles and (D) fluids containing paramagnetic particles.

Ferrofluids are the colloidal suspensions related to surface-modified magnetic nanoparticles (2–20 nm) dispersed in a fluid carrier (Fig. 1; [1]) [2–4]. The applicable fields are divided into some biomedical categories: the cancer treatment by hyperthermia [5], MRI contrast agent [6], drug delivery [7], DNA hybridization [8] and cell separation [9]. To achieve the ferrofluid behavior for a material, there exist two ways: in one of them the ferromagnetic materials can be heated until it reaches the liquid. However, they lose their ferromagnetic behavior because the Curie point is lower than the melting point [10]. The only exception, undercooled melts of Co-Pd alloys, found to show a magnetic phase transition in 1996 is of no technical importance concerning magnetic field controlled flows and related applications [10]. Another way is to synthesize a colloid using very fine particles.

The syntheses of magnetic fluids consist of two steps: (a) the preparation of the nanosized magnetic particles that can be produced by microemulsion [11], co-precipitation [12], ball milling [13], sonochemical [14], sol-gel [15] and thermal decomposition [16]. (b) The subsequent stabilization/dispersion of the

nanoparticles in various non-polar or polar carrier liquids [17], in which magnetic nanoparticles can be coated by some methods such as co-precipitation [12], core-shell [18,19], micro-emulsion [20,21] and then levitated in the carrier liquid. To obtain a stable ferrofluid, dispersants [22,23] must be chosen to match the dielectric properties of the carrier liquid. Various surfactants, e.g. sodium oleate, dodecylamine, sodium carboxy-methylcellulose, are usually used to enhance dispersibility in an aqueous medium [24].

Historically, the first magnetic nanoparticle used in magnetic fluids was magnetite (Fe_3O_4), in 1960 by NASA [25,26], but different types of magnetic material include the following: Ferrites: MFe_2O_4 ($M=Mn, Ni, Co, Zn, Fe$) [22,27,28], $\gamma-Fe_2O_3$ [29] and some alloys such as FePt, NiPt and NiPd [30,31], which can be used in the magnetic fluid. Although pure metals (Fe, Co, Ni) possess the highest saturation magnetization, they are highly toxic and extremely sensitive to oxidation then without a further appropriate surface treatment such pure metal nanoparticles are not relevant for biomedical applications [32]. In contrast, iron oxides are less sensitive to oxidation and, therefore, can give a stable magnetic response. In fact, small iron oxide nanoparticles have been applied to in vitro diagnosis for about 50 years. Recent studies have demonstrated that magnetite (Fe_3O_4) and maghemite ($\gamma-Fe_2O_3$) are very promising candidates due to their biocompatibility and relative ease to functionalize [33,34]. However, in order to achieve more safety for biomedical applications, iron oxide nanoparticles must be covered by an organic or inorganic biocompatible coating. These coatings include polyethylene glycol, polyethylene glycol fumarate, polyvinyl alcohol, acrylate-based coatings, dextran-based coatings, synthetic polyesters, alginate, chitosan and polyethylenimine, gold and silica [35].

* Corresponding author. Tel.: +98 711 7353509; fax: +98 711 7354520.
E-mail address: Shokrollahi@sutech.ac.ir (H. Shokrollahi).

By adding other ions such as Ni²⁺, Mn²⁺ and Co²⁺ to Fe₃O₄, ferrites having a range of magnetic properties can be obtained. This flexibility can be used to tune the magnetic properties for hyperthermia applications by creating cubic mixed-ferrite material. These ferrites have attracted special attention because they save time, have low inherent toxicity, ease of synthesis and their physical and chemical stabilities [36]. In all cases, however, issues of biocompatibility and toxicity limit the choice of materials; however, the use of coatings may make the use of these materials feasible.

It would be worth mentioning that due to the importance of biomedicine in our life, this paper investigates a physical concept of ferrofluids and the most important ferrites, which are regarded as magnetic cores used in the hyperthermia application.

2. Physical concepts of ferrofluids

2.1. Inter-particle interactions

An important factor in the application of ferrofluids is their colloidal stability. Stability is determined by the balance between

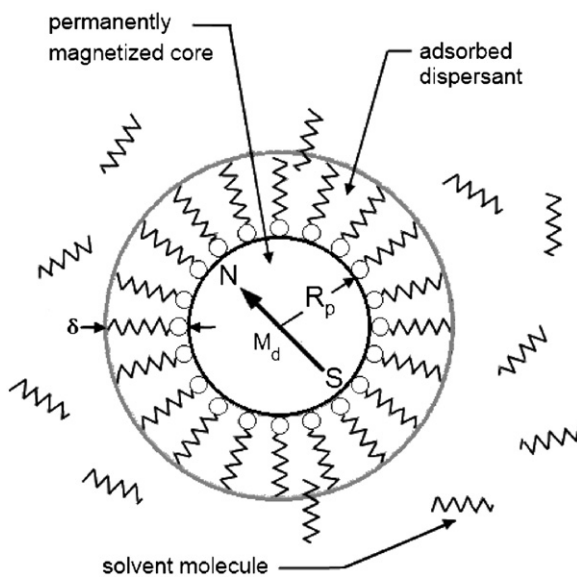


Fig. 1. Mechanism of the formation of colloidal suspension [1].

various forms of energy (attractive and repulsive forces) and thermal energy ($k_B T$) to avoid segregation over a period of time after the field is removed (Table 1). If the average thermal energy exceeds the sum of the total interactions (barrier energy) a negligible agglomeration will occur. Depending on the particle volume fraction, size distribution, temperature and applied magnetic field the aggregation will occur in ferrofluid [37].

When the A constant becomes zero means no agglomeration between the surfactant molecules will occur (similar dielectric properties between the carrier liquid and the tail). It can be shown that a surfactant layer of 2 nm thickness yields a steric repulsion strong enough to avoid the direct contact between the magnetic particles, thereby preventing the inter-particle agglomeration (Fig. 2) [10]. The steric repulsion force results from the reduction of the configuration room of the surfactant molecules, is much more short-ranged and operates at distances of the overlap of the surface layers. A surfactant layer consisting of long chain molecules with a polar head and an unpolar tail prevents the adhesion due to van der Waals forces. This force depends on the inter-particle distance and the thermal energy cannot re-disperse the particles being in contact.

Therefore, in the ferrofluids a relatively narrow distribution of small coated particles is important. The morphology and size of the coated magnetic particles of the different ferrofluids are shown in Fig. 3 [38,39]. From the TEM micrographs, it is obvious that the particles are nearly spherical in shape and are generally well dispersed.

2.2. Heat dissipation mechanisms

Heat dissipation from the small magnetic particles is caused by the delay in the relaxation of the magnetic moment through either the rotation within the particle (Néel) or the rotation of the particle itself (Brownian, viscous loss). These relaxation mechanisms are discussed when the magnetic particles are exposed to an AC magnetic field with the magnetic field reversal times shorter than the magnetic relaxation times of the particles. The Néel (τ_N) and Brownian (τ_B) magnetic relaxation times of a particle are given by the following equations [42,43]:

$$\tau_N = \tau_0 \exp(KV_M/k_B T) \tag{1}$$

$$\tau_B = \frac{3V_{hyd}}{k_B T} \eta \tag{2}$$

Table 1
Various forces acting in a ferrofluid [17, 37, 40, 41].

Interaction force	Equation	Ferrofluid stability criteria	Description	Particle type
Magnetic field energy	$ E_{mag} = \mu_0 M_0 V H$	$kT/\mu_0 M H V \geq 1, d \leq \left(\frac{6kT}{\pi\mu_0 M H}\right)^{1/3}$	(Attractive)	Uncoated particles
Gravitational field	$E_{grav} = \Delta\rho V g h$	$\frac{\Delta\rho g L}{\mu_0 M H} \ll 1$	Attractive	Uncoated particles
Dipole–dipole contact energy	$E_{dip} = (\mu_0 M_0^2/12)V.$	$\frac{12kT}{\mu_0 M^2 V} \geq 1, d \leq \left(\frac{12kT}{\pi\mu_0 M^2}\right)^{1/3}$	Attractive	Uncoated particles
Dipole–dipole un-contact energy	$v(r_{ij}, \mu_i, \mu_j) = v_{sr}(r_{ij}) + \frac{1}{r_{ij}^3} \left[\mu_i \mu_j - \frac{3(\mu_i \cdot r_{ij})(\mu_j \cdot r_{ij})}{r_{ij}^2} \right]$	-	Attractive	Uncoated particles
Van der Waals	$E_{vdw} = -\frac{A}{6} \left[\frac{2}{l^2 + 4l} + \frac{2}{(l+2)^2} + \ln\left(\frac{l^2 + 4l}{(l+2)^2}\right) \right]$	Thermal energy cannot re-disperse the particles being in contact and depends on the inter-particle distance	Attractive	Uncoated particles
Steric repulsion	-	It is much more short-ranged and operates at distances of the overlap of the surface layers	Repulsive	Coated particles

$\Delta\rho$: density difference between the particles and the carrier liquid, V : volume of a particle, H : external field, g : gravitational acceleration, h : typical height of the fluid container, μ_0 : magnetic constant, M_0 : spontaneous magnetization of the particle, μ_i : point dipole moment, r_{ij} : inter-particle distance, v_{sr} : isotropic short-range potential, A : Hamaker constant and l : distances between the particles.

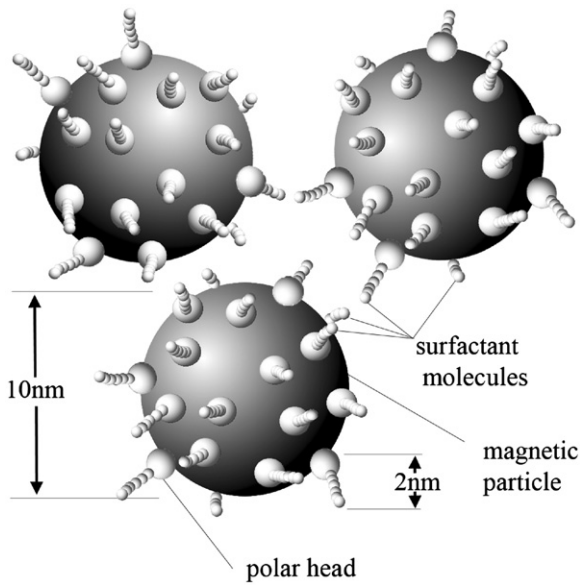


Fig. 2. Schematic representation of the coated magnetic particles in a ferrofluid. The size of the surfactant molecules has not been given on the scale to make the figure clearer [10].

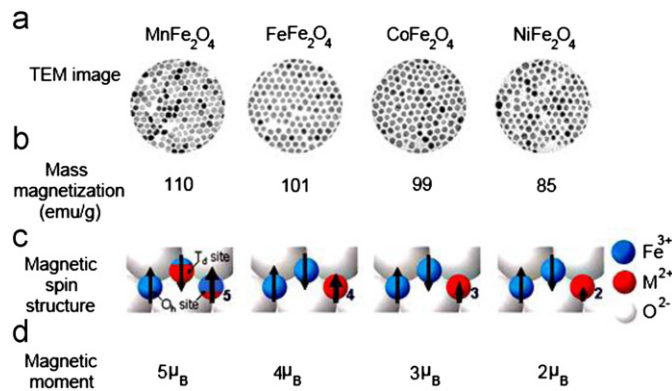


Fig. 3. Intrinsic magnetic properties for various uniformly sized spinel ferrite nanoparticles [39].

$$\tau_{eff} = \frac{\tau_B \tau_N}{\tau_B + \tau_N} \quad (3)$$

where τ_N is the Néel relaxation time, τ_B is the Brownian relaxation time, τ_{eff} is the effective relaxation time, τ_0 is approximately 10^{-9} s, K is the anisotropy constant, V_M is the volume of particle, k_B is the Boltzmann constant, T is the temperature, η is the viscosity and V_{hyd} is the hydrodynamic particle volume [42].

From the above equations, it is obvious that the relaxation time relies on the particle diameter. When the particles are exposed to an AC magnetic field with the time of magnetic reversals less than the magnetic relaxation times of particles, the heat is dissipated due to the delay in the relaxation of the magnetic moment. Thus, the heat dissipation value is calculated using the harmonic average of both relaxations and their relative contributions depending on the particle diameter [42]. For the superparamagnetic nanoparticles, the power loss is calculated from Eq. (4) [44], where m is the magnetic nanoparticles' (MNPs) magnetic moment, ω is the field angular frequency, H is the AC magnetic field amplitude and ρ is the ferrite density:

$$P = (mH\omega\tau_{eff})^2 / [2\tau_{eff}k_B T \rho V (1 + \omega^2 \tau_{eff}^2)] \quad (4)$$

3. Hyperthermia

Cancer treatment options include surgery, chemotherapy, radiation therapy and hyperthermia. Clinical hyperthermia falls into three broad categories, namely (1) localized hyperthermia, (2) regional hyperthermia and (3) whole-body hyperthermia. Heating (41–46 °C) of specific tissues or organs for tumor/cancer therapy is named hyperthermia and can be generated by radio frequency, microwave and laser wavelengths [45–47]. Blood vessels are poorly developed within the cancerous tissues and have a lower thermal resistance than healthy tissue. Tumor cells are considered more susceptible to heat than normal cells due to their higher rates of metabolism, which makes hyperthermia a very promising cancer treatment [32].

The cancer cell is damaged at lower temperatures than the healthy tissue but a small section of tumor may not be heated. The two most obvious reasons are either because of a locally increased level of blood flow, because of a nearby blood vessel, or an inadequate concentration of implanted magnetic nanoparticles.

The challenge in this method is to restrict local heating of the tumor surrounding by self-control heating or by lowering the exposure time. This goal can be partially accomplished by the physical phenomenon of losses. It is desirable to have a high specific loss power (SLP) heat generated per unit mass of MNPs, to achieve the desirable temperature rise enhancement with low MNP concentration. In addition to the field parameters, specific loss power of MNP dispersions are strongly dependent on particle size, size distribution, anisotropy constant, saturation magnetization and surface modification [46]. The magnetic material is designed to have a Curie temperature equal to the temperature required for hyperthermia.

It is concluded that the selection of synthesis method and ferrite chemistry strongly affect the hyperthermia treatment. The specific absorption rate (SAR) is expressed by Eq. (5) where C is the specific heat of ferrofluid and sample holder taken together, $\Delta T/\Delta t$ is the initial slope of the time dependent temperature curve, $m_{ferrite}$ is the total ferrite content in the fluid [45]. Fig. 4 depicts the Co–Zn ferrite nanoparticles have higher magnetization and magnetic heating loss than Mn–Zn ferrite nanoparticles (Eq. (4)). Hence Co–Zn ferrite particles can be effectively used for the preparation of temperature sensitive ferrofluid. The research work done by Giri et al. [45] on the investigation of different soft ferrites for hyperthermia applications is shown in Fig. 5.

Fig. 5a depicts as the magnetic field and magnetic moment increase the SAR parameter increases (Eq. (4)). Furthermore, Fig. 5b

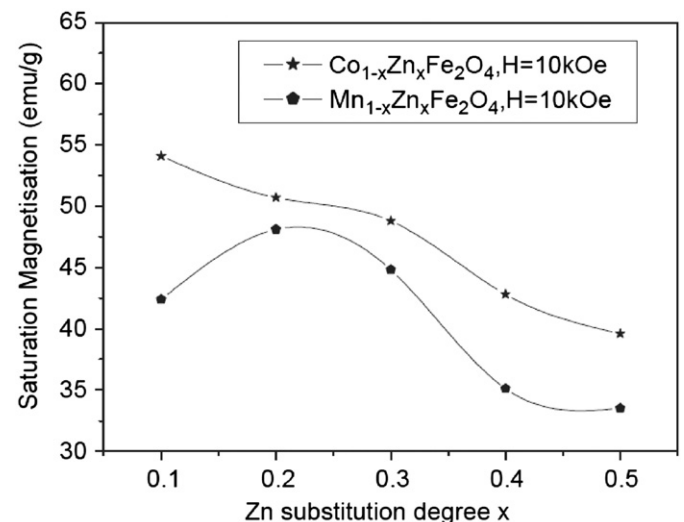


Fig. 4. Variation of saturation magnetization [65].

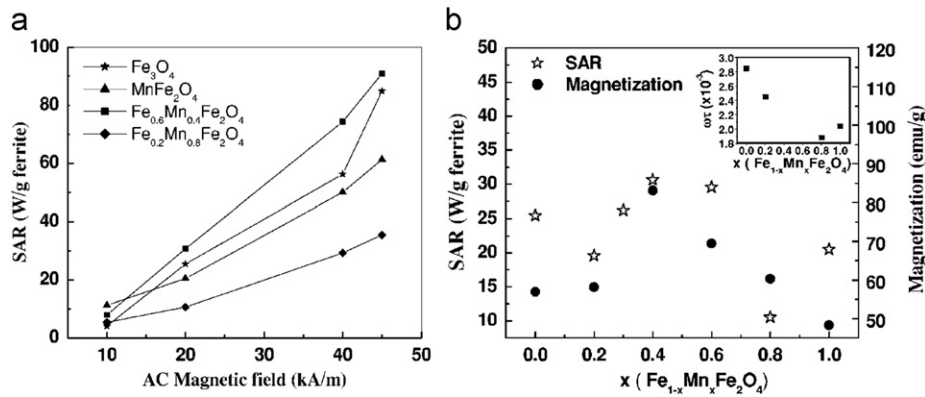


Fig. 5. Variation of SAR with (a) AC magnetic field amplitude measured at 300 kHz for different ferrofluid samples and (b) magnetization and Mn II concentration [45].

Table 2

Summary of relevant SAR determinations for ferrite nanoparticles [48–54].

Magnetic compound	Core diameter (nm)	Corona	H (kA/m)	ν (kHz)	SAR (W/g _{Fe})	Author/group
Magnetite	13	Aminosilan	13	520	146	Jordan/Felix (1999)
Magnetite	18	Dextran	16	55	57	Li-Ying/Xu-Man (2007)
Magnetite	10	–	6.5	400	211 ^a	Hilger/Kaiser (2001)
Magnetite	9–10	Lauric acid	15	300	168	Bahadur (2006)
Manganese ferrite	10–11	Lauric acid	15	300	135.8	Bahadur (2006)
Manganese ferrite	10	Liposomes	15	300	135	Pradhan/Bahadur (2007)
Cobalt ferrite	6	Mercaptoundecanoic acid (11-MUA)	50	266	6 ^a	Dong-Hyun/Brazel (2008)
Cobalt ferrite	18	Suspended in gel of agarose	30	108	3.5 ^a	Veverka/Vasseur (2007)
Cobalt ferrite	9–10	Lauric acid	15	300	51.8	Bahadur (2006)
Cobalt ferrite	15	Lauric acid, dodecylamine, 1,2- hexadecanediol	5	300	396.1	Dravid (2009)

^a (W/g_{Ferrite}).

Table 3

Different loss mechanisms under different average particle sizes.

Various conditions	$D > D_{SD}$	$D \sim D_{SD}^a$	$D_{SP}^b < D < D_{SD}$	$D \sim D_{SP}$	$D \leq D_{SP}^c$
Dominant loss mechanism/s	Hysteresis + Eddy current ^d + anomalous ^d	Hysteresis	Hysteresis + Néel + Brownian	Néel + Brownian	Brownian

^a Single domain diameter.

^b Superparamagnetic diameter.

^c In viscous medium.

^d At high frequency and high magnetic field.

shows the magnetization initially increases with x up to a value of $x=0.4$ and then it decreases. The decrease beyond $x=0.4$ is due to the weakening of the AB interaction when Fe³⁺ is substituted by Mn²⁺ in the A site. Table 2 compares the SAR results of the most widely used ferrite compounds. It is clear that the SAR value strongly depends on the particle size, surfactant of ferrite material. For example, in the case of Co-ferrite the highest value of SAR~396 can be related to the mono-dispersed particles synthesized by thermal decomposition method [48–54]. Table 3 summarizes the different magnetic heat generation mechanisms as a function of average particle size:

$$SAR = C \frac{\Delta T}{\Delta t} \frac{1}{m_{ferrite}} \quad (5)$$

4. Magnetic properties of nanosized particles

The change in magnetic properties of small ferrite particles such as M_S , H_C and Curie temperature is due to the influence of the surface effects, cationic stoichiometry and their occupancy in the

specific sites [55]. Magnetic particles below a critical diameter cannot support more than one domain, and are thus described as “single domain”. This critical diameter is approximately $2A^{1/2}/M_S$ (A : exchange constant, M_S : moment per unit volume), and typically is about 10–100 nm for a wide range of materials. In here, the different effective parameters on the magnetic properties of nanosized particles will be explained.

4.1. Size effect

Magnetic properties of nanomaterials change as the ratio of surface to volume increases. Formation of dead layer on the surface, existence of random canting of particle surface spins, non-saturation effect due to random distribution of particle size, deviation from the normal cation distribution/cation site disorder, presence of adsorbed water also result in the reduction of magnetic properties of nanosized particles.

Fig. 6 illustrates as the particle size decreases the coercivity increases up to single domain region and then decreases as a result of superparamagnetic size ($H_C \sim 0$) [20]. Magnetic nanoparticles display the phenomenon of superparamagnetism, not